On closely coupled dipoles with load matching in a random field

Lau, Buon Kiong; Bach Andersen, Jørgen

Published in:
2006 IEEE 17th International Symposium on Personal, Indoor and Mobile Radio Communications (IEEE Cat. No. 06TH8881)

DOI:
10.1109/PIMRC.2006.254018

2006

Document Version:
Peer reviewed version (aka post-print)

ON CLOSELY COUPLED DIPOLES WITH LOAD MATCHING IN A RANDOM FIELD

Buon Kiong Lau
Department of Electroscience
Lund University
Box 118, SE-221 00 Lund
Sweden
bklau@ieee.org

Jørgen Bach Andersen
Department of Communications Technology
Aalborg University
Niels Jernes Vej 12 A5, 9220 Aalborg Ø
Denmark
jba@kom.aau.dk

ABSTRACT

MIMO is a wireless communication technology that is growing in popularity due to its ability to deliver significant improvements over conventional systems. However, some applications require antennas to be closely spaced, which results in strong coupling among the antennas and performance degradation. Here we show that in a random field, load impedance can play an important role in the power, correlation and capacity performance of MIMO systems. While a good choice of load impedance can alleviate the loss of power and correlation performance, capacity performance is less sensitive to load variation. Moreover, the phase component of open circuit correlation has been found to have a significant influence on MIMO performance, indicating that important information is lost if it is neglected. A comparison between the performance metrics over different load impedances indicates that capacity depends largely on received power and not correlation.

I. INTRODUCTION

Although the MIMO technology can be traced as far back as [1], it was not until the late 1990's that it started to attract a great deal of academic interest [2]-[4]. Albeit significant breakthroughs, successful standardization and commercialization (in wireless LANs), MIMO research continues to present both interesting and important challenges. One such challenge is the implementation of MIMO in small platforms, such as a mobile handset. This is because one necessary condition for MIMO gains is sufficiently low antenna correlation at both the transmit *and* receive antenna arrays. Conventionally, this requirement sets the lower limit on antenna separation distance. Moreover, the lower antenna system efficiency resulting from impedance mismatch of closely coupled antennas further reduces MIMO gains [5], [6].

A recent work reveals that a simple matching load (or an uncoupled matching network) can have a remedial effect on the aforesaid phenomena [7]. In fact, the load can be chosen to result in low or zero output correlation for a given random field in which the antennas reside. However, it is also evident that some tradeoffs are necessary between the criteria of antenna correlation and antenna system efficiency. The existence of two maxima in received power over different load impedances is also an interesting feature for closely coupled antennas [7], In fact, the double maxima appeared earlier in [8], though [8] assumes real-valued antenna and load impedances.

On the other hand, the so-called multiport conjugate match is able to retain both zero output correlation and 100% efficiency for any antenna separation [5], [9]. However, this ideal behaviour can only be achieved in a narrow frequency band, in the limit of small antenna separation, due to basic limitations in matching network [9], [10] .

In this paper, we consider several extensions to the previous work in [7]. First, we investigate the impact of simple matching on capacity. The capacity criterion is important, as it represents the theoretical limit for communications over a noisy channel, and is a function of both efficiency and correlation. Second, we consider the impact of complex open circuit (OC) correlation resulting from asymmetrical angular power spectrum (APS) about the broadside of the receive array. The impact of asymmetrical spectrum was the subject of [11]. However, [11] did not consider the impact of matching impedance. Finally, we show that for the cases examined, capacity is a strong function of received power, and is less influenced by correlation.

In Section II, we present the MIMO system model used in our study. This is followed by the formulation of received power, correlation and capacity in Section III. Section IV demonstrates numerically the impact of load impedance and random field on received power, correlation and capacity, and the relationship between these criterions for different load impedances. We conclude the paper in Section V.

II. MIMO SYSTEM MODEL

A simplified model of a $M \times N$ MIMO system consists of M transmit circuits, a propagation channel, and N receive circuits. We consider here the case of half-wavelength ($\lambda/2$) electric dipole antennas. The m-th transmit circuit consists of voltage source V_{Sm}, source impedance Z_{Sm} and a dipole antenna, whereas a dipole antenna terminated with load impedance Z_{Ln} makes up the n-th receiver circuit.

To simplify the analysis, we study a 2×2 MIMO system of identical thin dipole antennas and identical source ($Z_S = Z_{S1} = Z_{S2}$) and load ($Z_L = Z_{L1} = Z_{L2}$) impedances. The focus is on the receive end. In other words, we assume that the requirement for small antenna separation d is on the receive end, i.e., downlink transmission. The circuit equivalent of the receive

This work was supported by VINNOVA (grant no. P24843-3) and partly conducted within the Network of Excellence NEWCOM (Network of Excellence in Wireless Communications).

subsystem is given in Fig. 1, where V_{oc1}, V_{oc2} denote open-circuit voltages of antennas 1 and 2, respectively, Z_{11} the self impedance of antenna 1 (or antenna 2) and Z_{12} the mutual impedance between antennas 1 and 2. For the transmit subsystem, the circuit diagram is equivalent to Fig. 1, with V_{oc1}, V_{oc2} replaced by V_{S1}, V_{S2} and Z_S by Z_L. However, the two transmit antennas are assumed to be far apart and have negligible mutual coupling, i.e. $Z_{12} = 0$. We further assume conjugate matching for the source impedance, i.e., $Z_S = Z_{11}^*$.

On the transmit side, the excitation current is given by

$$\begin{bmatrix} I_{S1} \\ I_{S2} \end{bmatrix} = \frac{1}{2\,\mathrm{Re}(Z_{11})} \begin{bmatrix} V_{S1} \\ V_{S2} \end{bmatrix}. \tag{1}$$

The excitation currents are sources of radiation from the antennas and since they are sufficiently separated, the transmit antenna correlation is zero. On the receive end, however, the open circuit voltages are highly correlated (with correlation α) due to the small antenna separation. In the case of uniform 2D APS, $\alpha = J_0(kd)$, where $J_0(\bullet)$ is the Bessel function of the first kind of order 0, $k = 2\pi/\lambda$ the wavenumber and d the antenna separation. Using the well-established Kronecker model, the propagation channel can be represented as

$$\mathbf{H}_{Ch} = \mathbf{\Psi}_R^{1/2} \mathbf{H}_{iid} (\mathbf{\Psi}_T^{1/2})^T, \tag{2}$$

where $$\mathbf{\Psi}_R = \begin{bmatrix} 1 & \alpha \\ \alpha^* & 1 \end{bmatrix},$$

and $\mathbf{\Psi}_T = \mathbf{I}$ (identity matrix) are the receive and transmit correlation matrices, respectively, each entry of the 2 × 2 matrix $\mathbf{H}_{iid}$ is a complex Gaussian random variable of zero mean and average power of 1.

At the receive subsystem (see Fig. 1), the excitation sources are the open circuit voltages. The current at each circuit is given by

$$\begin{bmatrix} I_{L1} \\ I_{L2} \end{bmatrix} = \underbrace{\left(Z_L \mathbf{I} + \begin{bmatrix} Z_{11} & Z_{12} \\ Z_{12} & Z_{11} \end{bmatrix} \right)^{-1}}_{\mathbf{Z}} \begin{bmatrix} V_{oc1} \\ V_{oc2} \end{bmatrix}. \tag{3}$$

The output (or load) voltage is then

$$\begin{bmatrix} V_{L1} \\ V_{L2} \end{bmatrix} = Z_L \mathbf{I} \begin{bmatrix} I_{L1} \\ I_{L2} \end{bmatrix}. \tag{4}$$

III. Performance Metrics

Antenna correlation has been used extensively to measure diversity gain [8]. More recently, improved measures, such as the effective diversity gain [6], are used to include both correlation effect and radiation efficiency of the antennas. The correlation and received power metrics are described in [7], except that here we consider the *total* average received power from both receive antennas.

The expression for MIMO capacity (assuming no CSI at the transmitter) is given by

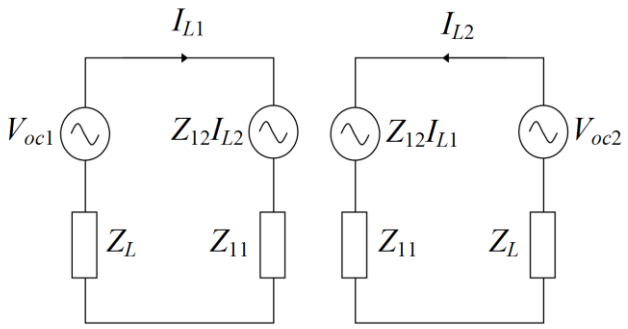

Fig. 1. Equivalent circuit for receive end.

$$\begin{aligned} C &= \log_2 \det\left(\mathbf{I} + \frac{\gamma_{ref}}{MP_s} \mathbf{H}\mathbf{Q}\mathbf{H}^H \right) \\ &= \log_2 \det\left(\mathbf{I} + \frac{\gamma_{ref}\, 4\,\mathrm{Re}(Z_{11})\mathrm{Re}(Z_L)}{M} \mathbf{Z}^{-1}\mathbf{H}_{Ch}\left(\mathbf{Z}^{-1}\mathbf{H}_{Ch}\right)^H \right), \end{aligned} \tag{5}$$

where $\mathbf{Q} = P_{in}\mathbf{I}$, $P_{in} = 2\,\mathrm{Re}(Z_{11})|I_{S1}|^2$, γ_{ref} the reference SNR, $\mathbf{H}$ the overall channel or transfer function matrix between the transmit sources and the receive loads, P_s the average received power for a single antenna system with conjugate impedance match at both the source and load impedances (used to normalize $\mathbf{H}$). Since the transmit circuits are assumed to be completely decoupled and each conjugate-matched, as in the single antenna case, the capacity expression (5) measures relative difference at the receive end only. The validity of the expression has been verified against the S-parameter approach of [5]. Both approaches were found to give identical results.

IV. Parametric Study and Discussions

In this section, we provide a numerical study of the impact of load impedance and the APS-dependent OC correlation on output correlation, received power and capacity for closely coupled dipoles. We assume thin dipoles with $Z_{11} = 73.1 + j43$ and $Z_{12} = 71.7 + j24.3\Omega$, $67.3 + j7.6\Omega$ at $d = 0.05\lambda, 0.1\lambda$, respectively.

A. Effect of Real OC Correlation on MIMO Capacity

Earlier results in [7] and [8] focused on real-valued OC correlations. The plots of received power and (magnitude of) output correlation ρ for uniform 2D APS over different load impedances were given in [7] for $d = 0.05\lambda$. In Fig. 2, we show the contour plot of the mean capacity for this case. The capacity distribution is calculated from (5) using 2000 realizations of $\mathbf{H}_{iid}$ and for $\gamma_{ref} = 20$ dB. The capacity contour bears a closer resemblance to that of the received power than the output correlation in [7], a point which will be followed up in Section IV-D. Nevertheless, unlike the received power, the capacity has only one maximum. The maximum at the broad matching area [7] disappeared in the capacity contour due to high correlation in that region. The position of the narrow peak (at $Z_L = 1.53 - j18.73\Omega$) in the received power has been shifted to the right due to the

contribution of low to zero correlation to capacity improvement in this region. It is noted that the narrow received power peak demonstrates the so-called super-directivity characteristics [12], with maximum zero-spread directivity 6.23 dBi at ±90° (see Fig. 3). Interestingly, super-directivity is also a feature of the more complicated multiport conjugate match [13], [14].

For comparison, the mean capacity of uncorrelated Rayleigh channels for 2 × 2 MIMO and SNR of 20 dB is 11.28 bits/s/Hz. Therefore, in the best case, the closely coupled configuration suffers performance degradation of 2.7 bits/s/Hz as compared to the ideal case. However, since the conjugate-matched single antenna system gives a mean capacity of 5.9 bits/s/Hz, the two-antenna MIMO system can in most cases give a capacity gain in excess of 1.5 bits/s/Hz over the single antenna system.

B. Effect of Complex OC Correlation on Received Power, Output Correlation and Capacity

In general, the OC correlation is a complex number. This occurs when the 2D APS is asymmetrical about the broadside of the receive array. Such a distribution can be conveniently formed by adding an offset to a symmetrical distribution, such as the Gaussian distribution [11]. Here we use the Laplacian distribution, as it gives a better fit to existing measurement results [15]

$$p(\phi) = c_1 \exp\left[-\sqrt{2}\left|\phi-\phi_0\right|/\sigma\right]\Big/\sqrt{2}\sigma\,, \qquad (6)$$

where ϕ_0 and σ are respectively the mean and the standard deviation of the distribution, c_1 is a normalization factor such that the integral of $p(\phi)$ over the azimuth plane is 1.

The OC correlation α can be calculated for different values of ϕ_0 and σ using (6) and the isolated single antenna pattern $g(\phi)$

$$\alpha = \int_{-\pi}^{\pi} E_{oc1}(\phi) E_{oc2}^{*}(\phi)\, p(\phi) d\phi \Big/ \int_{-\pi}^{\pi} \left|E_{oc1}(\phi)\right|^2 p(\phi) d\phi\,, \quad (7)$$

where $\left|E_{oc1}(\phi)\right| = \left|E_{oc2}(\phi)\right|$, $E_{oc1}(\phi) = g(\phi)\exp(-j\pi d\sin\phi)$ and $E_{oc2}(\phi) = g(\phi)\exp(j\pi d\sin\phi)$ for identical dipoles (see Fig. 4). Two different Laplacian APS are chosen on the curve $|\alpha|$ = 0.98, i.e. $(\phi_0,\sigma) = \{(0^\circ, 20.6^\circ), (90^\circ, 40.6^\circ)\}$ (marked by crosses), corresponding to $\alpha = 0.98\angle 0^\circ$ and $0.98\angle 29.1^\circ$, respectively. The received power, the magnitude of output correlation ρ, and mean capacity corresponding to these two scenarios are given in Figs 5-10.

The different complex OC correlations of the same absolute value can be observed to give different results. Comparing between Figs. 5 and 8, we note that the phase component of the OC correlation result in significant difference in the received power contour, where in Fig. 5 the maximum of ≈ 0.3 dB occurs at $Z_L \approx 130 - j50$, and in Fig. 8 ≈ 3 dB at $Z_L \approx 8 - j35\Omega$.

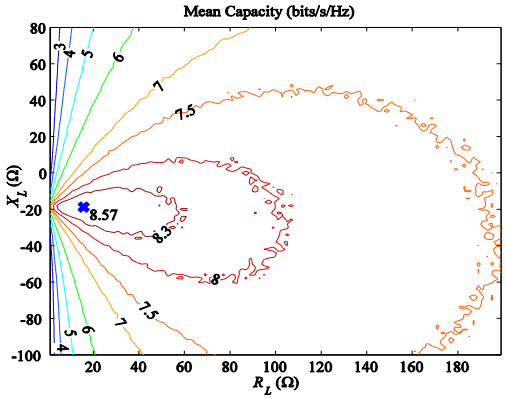

Fig. 2. Mean capacity for uniform 2D APS and $d = 0.05\lambda$.

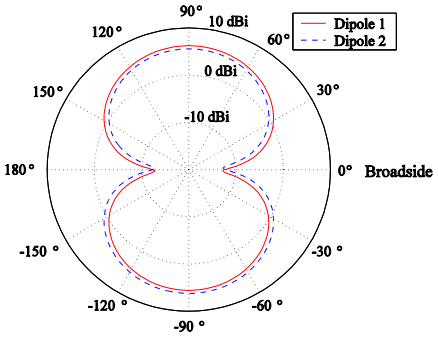

Fig. 3. Dipole antenna patterns with $Z_L = 1.53 - j18.73\Omega$ at $d = 0.05\lambda$.

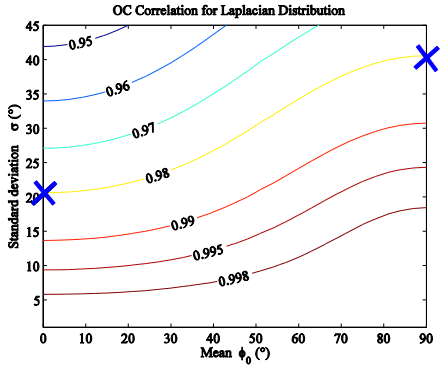

Fig. 4. OC correlation of Laplacian distribution for $d = 0.1\lambda$.

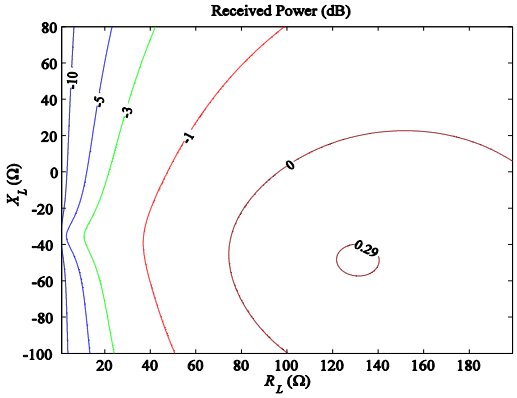

Fig. 5. Received power for $(\phi_0,\sigma) = (0^\circ, 20.6^\circ)$ and $d = 0.1\lambda$.

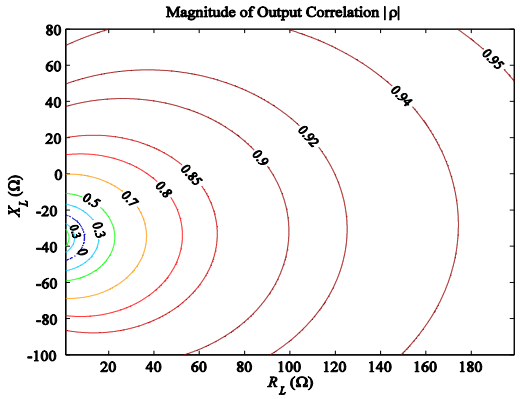

Fig. 6. Output correlation for $(\phi_0,\sigma)=(0^\circ,20.6^\circ)$ and d = 0.1λ.

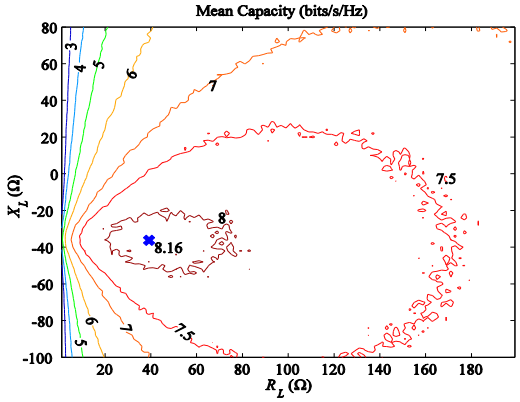

Fig. 7. Mean capacity for $(\phi_0,\sigma)=(0^\circ,20.6^\circ)$ and d = 0.1λ.

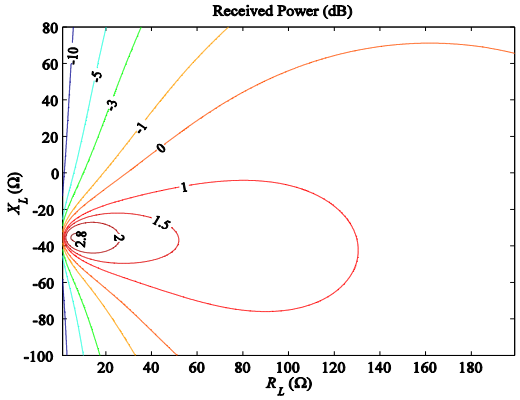

Fig. 8. Received power for $(\phi_0,\sigma)=(90^\circ,40.6^\circ)$ and d = 0.1λ.

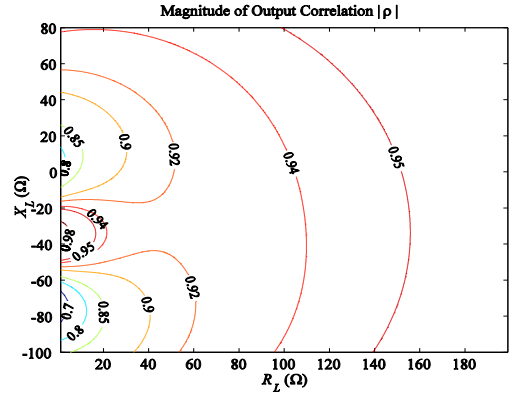

Fig. 9. Output correlation for $(\phi_0,\sigma)=(90^\circ,40.6^\circ)$ and d = 0.1λ.

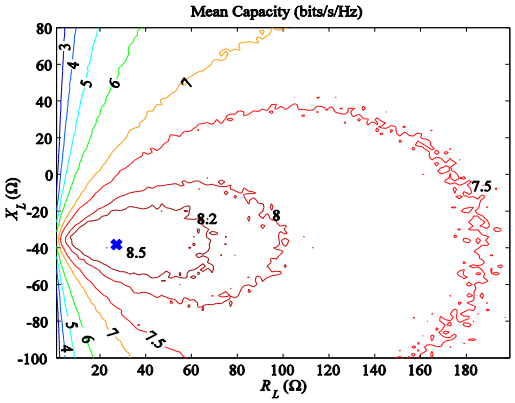

Fig. 10. Mean capacity for $(\phi_0,\sigma)=(90^\circ,40.6^\circ)$ and d = 0.1λ.

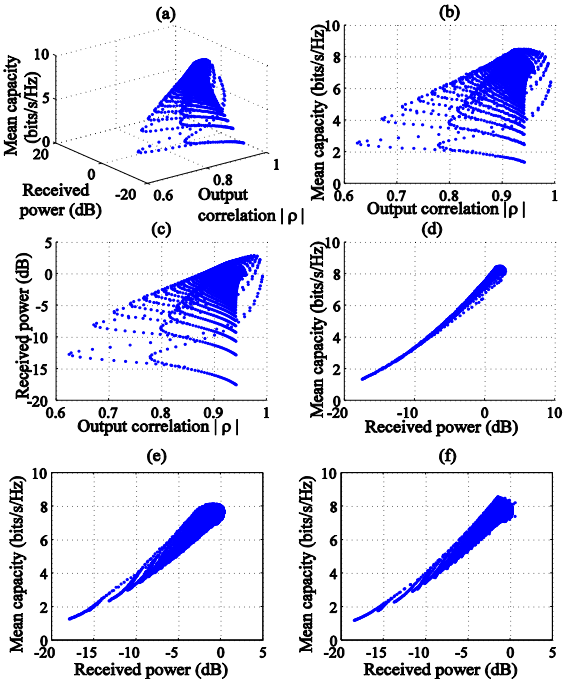

Fig. 11. (a) 3D plot of output correlation, received power and mean capacity for different load impedances; (b) Mean capacity vs. output correlation for $(\phi_0,\sigma)=(90^\circ,40.6^\circ)$; (c) Received power vs. output correlation for $(\phi_0,\sigma)=(90^\circ,40.6^\circ)$; Mean capacity vs. received power for (d) $(\phi_0,\sigma)=(90^\circ,40.6^\circ)$, (e) $(\phi_0,\sigma)=(0^\circ,20.6^\circ)$, and (f) uniform 2D APS and d = 0.05λ.

The large 3 dB power gain in Fig. 8 can be explained by the super-directive antenna pattern at this load impedance, which is similar to that of Fig. 3. The Laplacian APS centered at 90° (array endfire) aligns with the direction of maximum directivity and thus collected power is maximized. In other words, the limited angular spread of the APS emphasizes the super-directive behavior. Moreover, due to the small amplitude difference and nearly 180° phase difference between the super-directive patterns of the two dipoles, very high and strongly negative output correlation of $\approx 0.976\angle 147^\circ$ is observed.

The different output correlation contours between the two cases in Figs 6 and 9 is particularly obvious around the region of super-directivity, where the symmetrical APS gives very low output correlation. This is because even though the amplitude difference is small, the phase difference is larger in

the broadside region. Therefore, low to zero correlation values may be obtained.

The mean capacity contours of Figs. 7 and 10 are more similar in feature than the corresponding results of output correlation and received power. This is due to both received power and output correlation contributing to capacity, resulting in the capacity peaks appearing in between the maxima of the received power and correlation contours. It should be noted, however, that the maximum capacities differ between the two cases, where it is 8.16 bits/s/Hz in Fig. 7 and 8.5 bits/s/Hz in Fig. 10. The latter case is a direct result of larger relative collected power for the asymmetrical APS.

These results highlight the limitations of considering only the amplitude of the OC correlation α, where any difference in the unaccounted phase angle can change received power, output correlation and capacity quite dramatically. This indicates that important information is lost when one approximates the OC correlation only by its amplitude, at least in the cases shown here. Moreover, we note that output correlation is a poor predictor of mean capacity. A case in point is by comparing Figs. 6 and 7, where the mean capacity varies between 3 and 8 bits/s/Hz on the curve $|\rho| = 0.8$.

C. Relationship Between Output Correlation, Received Power and Mean Capacity

To examine if any relationship exists among output correlation, received power and mean capacity over the investigated range of load impedances, we plot in Fig. 11(a) the 3D graph of these quantities based on results in Figs. 8-10. Each data point corresponds to a load impedance Z_L. As can be seen, capacity appears to be strongly dependent on the received power, while no apparent connection is seen between other pairs of quantities. Indeed, 2D plots of every pair of the three quantities in Figs. 11(b)-(d) confirm this observation. However, it should be noted that output correlation plays a greater role in determining the capacity (within a range of 1 bits/s/Hz) at higher received powers than at lower received powers. In Figs. 11(e) and (f), the relationship between received power and mean capacity is also investigated for $(\phi_0, \sigma) = (0^\circ, 20.6^\circ)$ and $d = 0.1\lambda$ (i.e. Figs. 5 and 7), and uniform 2D APS and $d = 0.05\lambda$ (Section IV-A), respectively. The strong dependence of capacity on received power is also seen in these cases.

The above results suggest that for closely coupled dipoles with simple load impedance match, capacity is maximized when the received power is at its maximum. Nevertheless, it is important to recognize that the minor role of output correlation in determining capacity is attributed to the predominantly high output correlations in these cases, as can be seen from the correlation plot in [7], Figs. 6 and 9. It is well established that envelope correlation ρ_e = 0.5 or complex correlation $|\rho| \approx \sqrt{\rho_e}$ = 0.707 is the rule of thumb for good diversity gain. It can be seen from Fig. 9 that good diversity gain can hardly be achieved for any load impedances, resulting in the dominance of received power in the capacity performance in Fig. 11(d).

V. CONCLUSIONS

In this paper, we showed that simple impedance matching can play a significant role in the resulting MIMO performance metrics of received power, output correlation, and mean capacity. The presence of super-directivity and its impact on MIMO performance is also demonstrated.

Different complex OC correlations of the same absolute value have been found to give different results for the aforesaid metrics, indicating that significant discrepancies can arise from neglecting the phase of complex correlations. Whereas no obvious relationship can be found between received power and output correlation, as well as between output correlation and capacity, a strong link is observed between received power and capacity. As a result, good capacity performance can be expected from optimizing load impedance for maximum received power. Finally, we note that the paper only looks into mean capacity. Outage capacity may give different conclusions.

REFERENCES

[1] J. Winters, "On the Capacity of Radio Communication Systems with Diversity in a Rayleigh Fading Environment," *IEEE J. Select. Areas Commun.*, vol. SAC-5, pp.871-878, Jun. 1987.

[2] I. E. Telatar, "Capacity of multi-antenna Gaussian channels," *European Trans. Telecommun.*, vol. 10, pp. 585-595, 1999.

[3] G. J. Foschini and M. J. Gans, "On limits of wireless communications in a fading environment when using multiple antennas," *Wireless Personal Communications* (Kluwer Academic Publishers), vol. 6, pp. 311–335, Mar. 1998.

[4] S. N. Diggavi, N. Al-Dhahir, A. Stamoulis, and A. R. Calderbank, "Great expectations: The value of spatial diversity in wireless networks," *Proc. IEEE*, vol. 92, pp. 219-270, Feb. 2004.

[5] J. W. Wallace and M. A. Jensen, "Mutual coupling in MIMO wireless systems: a rigorous network theory analysis," *IEEE Trans. Wireless Commun.*, vol. 3, no. 4, pp. 1317-1325, Jul. 2004.

[6] P. S. Kildal and K. Rosengren, "Electromagnetic analysis of effective and apparent diversity gain of two parallel dipoles," *IEEE Antennas and Wireless Propagat. Lett.* , vol. 2, no. 1, pp. 9-13, 2003.

[7] J. B. Andersen and B. K. Lau, "On closely coupled dipoles in a random field," *IEEE Antennas and Wireless Propagat. Lett.*, vol. 5, no. 1, pp. 73-75, 2006.

[8] R. G. Vaughan and J. B. Andersen, "Antenna diversity in mobile communications," *IEEE Trans. Vehic. Technol.*, vol. VT-36, no. 4, pp. 149-172, Nov. 1987.

[9] B. K. Lau, S. M. S. Ow, G. Kristensson, and A. F. Molisch, "Capacity Analysis for Compact MIMO Systems", in *Proc. IEEE 61st VTC Spring*, vol. 1, pp. 165-170, Stockholm, Sweden, 2 May-1 Jun. 2005.

[10] B. K. Lau, J. B. Andersen, G. Kristensson, and A. F. Molisch, "Impact of Matching Network on Bandwidth of Compact Antenna Arrays," *IEEE Trans. Antennas Propagat.*, to be published.

[11] X. Lie and Z. Nie, "Mutual coupling effects on the performance of MIMO wireless channels," *IEEE Antennas Wireless Propag. Lett.*, vol. 3, pp. 344-347, 2004.

[12] R. Harrington, "Antenna excitation for maximum gain," *IEEE Trans. Antennas Propagat.*, vol. AP-13, pp. 896-903, Nov. 1965.

[13] S. Dossche, S. Blanch, and J. Romeu, "Three different ways to decorrelate two closely spaced monopoles for MIMO applications," in *Proc. IEEE/ACES Int. Conf. Wireless Commun. and Appl. Comput. Electromagnetics*, pp. 849-852, Honolulu, HI, 3-7 Apr. 2005.

[14] H. J. Chaloupka, X. Wang, and J. C. Coetzee, "A superdirective 3-element array for adaptive beamforming," *Microwave Opt. Tech. Lett.*, vol. 36, pp. 425-430, Mar. 2003.

[15] A. F. Molisch, *Wireless Communications*, Wiley, 2005.